Analysis on regulation strategies for extending service life of hydropower turbines

W Yang [1,2], P Norrlund [1,3], J Yang [2]

[1] Department of Engineering Sciences, Uppsala University, Uppsala, SE-751 21, Sweden
[2] The State Key Laboratory of Water Resources and Hydropower Engineering Science, Wuhan University, Wuhan, 430072, China
[3] Vattenfall R&D, Älvkarleby, SE-814 26, Sweden

Corresponding author's e-mail: Weijia.Yang@angstrom.uu.se (W Yang)

Abstract. Since a few years, there has been a tendency that hydropower turbines experience fatigue to a greater extent, due to increasingly more regulation movements of governor actuators. The aim of this paper is to extend the service life of hydropower turbines, by reasonably decreasing the guide vane (GV) movements with appropriate regulation strategies, e.g. settings of PI (proportional-integral) governor parameters and controller filters. The accumulated distance and number of GV movements are the two main indicators of this study. The core method is to simulate the long-term GV opening of Francis turbines with MATLAB/Simulink, based on a sequence of one-month measurements of the Nordic grid frequency. Basic theoretical formulas are also discussed and compared to the simulation results, showing reasonable correspondence. Firstly, a model of a turbine governor is discussed and verified, based on on-site measurements of a Swedish hydropower plant. Then, the influence of governor parameters is discussed. Effects of different settings of controller filters (e.g. dead zone, floating dead zone and linear filter) are also examined. Moreover, a change in GV movement might affect the quality of the frequency control. This is also monitored via frequency deviation characteristics, determined by elementary simulations of the Nordic power system. The results show how the regulation settings affect the GV movements and frequency quality, supplying suggestions for optimizing the hydropower turbine operation for decreasing the wear and tear.

1. Introduction

In recent years, there is a tendency that the hydropower turbines experience a greater extent of fatigue, due to more frequency regulation movements caused by increasingly more integration of intermittent renewable energy sources, e.g. wind and solar [1,2]. Therefore, the purpose of this paper is to extend the service life of hydropower turbines, by reasonably decreasing the guide vane (GV) movements with appropriate regulation strategies. However, different regulation strategies influence the active power output and then affect the power system frequency. Therefore the regulation performance, which is reflected by the frequency quality of the power system, is also an important focus of this study.

This study is based on the previous works [3] and [4], where the detailed research background and literature reviews can be found. In the hydraulics research field, two recent reviews introduce the hydro turbine failure mechanisms [5] and fatigue damage mechanism [6]. Regarding Francis turbines, the dynamic loads [2,7], fatigue design and life of runners [8-10] has been examined. For Kaplan turbines, the influence of primary control to the

residual service life of runners has been studied [11]; the pressure at discharge control and frequency control has been investigated to analyse the life time of high head runners and low head runners [1]; Failure analysis of the shaft of a 28 MW Kaplan turbine has been conducted [12]. In this study, the research objective is only Francis turbines.

The main method follows the approaches in [3,4]. Two very important indicators for wear and tear of turbines, accumulated distance and amount of guide vane movements, are applied throughout this paper, as shown in Figure 1. This work also adopts the scope and assumptions found in Section 2 of [3]. Here, it is necessary to underline that, there is no quantitative prediction of turbine service life in this work, only the qualitative analysis is considered: more distance and amount of GV movements indicate more wear and tear, signifying shorter service life.

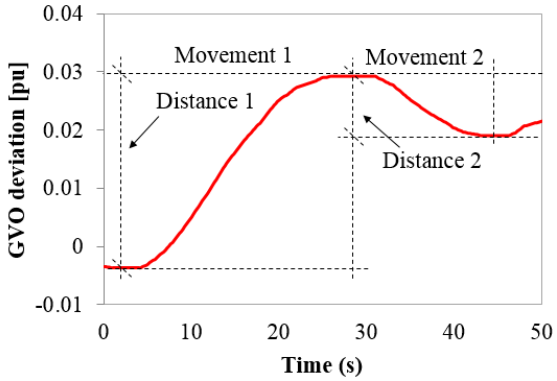

Figure 1 [3]. Changing process of guide vane opening, illustrating two important indicators: distance and amount of guide vane movements, larger values of them indicate more wear and tear of turbines

The content of this paper is organized as follows: In Section 2, methods and models for both numerical simulation and basic theoretical formulas are presented. In Section 3, the simulation results and the formula calculations are showed and discussed. The conclusions are condensed in Section 4.

2. Methods and models

The methods and models are introduced in this section. Numerical simulation based on MATLAB/Simulink is the main approach in this study, for computing the guide vane opening (GVO) and examining the frequency quality under various parameter settings. Basic theoretical formulas derived in [3] are also discussed and compared to the simulation results, to analyse the influence of different parameters on GV movement distance.

2.1 Numerical simulation

In this subsection, firstly, a model of a Francis turbine governor is presented. The distance and amount of GV movements can be obtained from the time-domain simulation result through statistics work. Secondly, a simple verification of the governor model is conducted based on on-site measurements in a Swedish hydropower plant (HPP). In the third place, models of the Nordic power system and the "inverse system" [4,13] are introduced for analysing the frequency quality of power systems. Fourthly, two main inputs of simulations are also described: the measured one-month frequency of the Nordic power system and the simulated load disturbance.

2.1.1 Governor model

In order to simulate the GVO process and conducting statistics of the two indicators, a governor model with high accuracy is needed. A Simulink model of a general turbine governor with different filters is shown in Figure 2. The nonlinear relation between GV servomotor stroke and GVO, due to that the linear servo motion is transferred to an angular motion, is ignored, implying that the final output after the servo is equivalent to the GVO. This simplification is acceptable because the influence of the nonlinearity is small in is study.

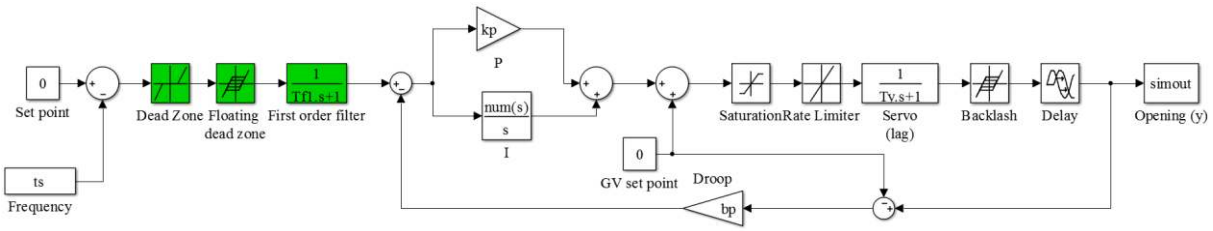

Figure 2. The Simulink model of a general PI (proportional-integral) governor with different filters, for computing GV movements. The filters in series, highlighted by green, are applied individually in the simulation. When one filter is in function, the setting values of other filters are 0.

Three types of controller filters [4], i.e. dead zone [14,15], floating dead zone [16] and linear filter [17] are included in this study. In the Simulink model, the implementation of the floating dead zone is actually the same as the backlash [15], and the first-order linear filter is described as

$$F_f(s) = \frac{1}{T_f \cdot s + 1}. \tag{1}$$

In this paper, the parameter T_f is known as the filter time constant, and K_p, K_i and b_p are governor parameters. The setting values of dead zone, floating dead zone are E_{dz} and E_{fdz} respectively. In the real power plants, the value of the filters can be altered manually, while the values of lag, backlash and delay block are fixed due to the mechanical characteristics of the system. This governor model is similar to the models in [3] and [4], the main revision here is that the feedback signal is taken from the final GVO value after the backlash and the delay.

2.1.2 Verification of governor model based on on-site measurements

The governor model is simply verified by comparing the simulated GVO and the on-site measurement data from a recently refurbished unit in a HPP owned by Vattenfall, the largest hydropower owner and operator in Sweden. The measurement was conducted in the spring of 2015 during normal operation, and the length is 3885 seconds. The GVO was measured through two approaches, as shown in Figure 3. The wire transducer and angular transducer were applied on two GVs (No.1 and No.2) separately.

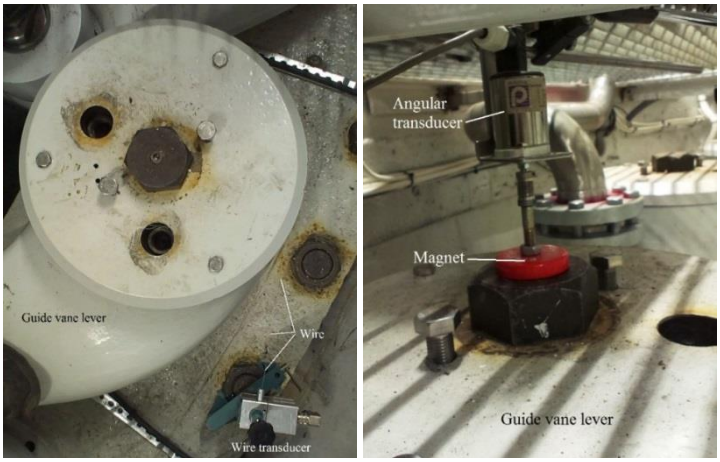

Figure 3. Left figure: Installation of wire transducer on the lever of GV No. 1. The wire is attached to the rim of a cylindrical part of the lever.

Right figure: Installation of angular transducer on GV No. 2. The magnet is centred on the bolt connecting the lever to the stem.

Figure 4 demonstrates the comparison between the simulation and the measurement. The measured GVO value is the average of two signals from GV No.1 and No.2. The frequency is obtained through a frequency transducer in the HPP. The sampling time of the signals is 0.2 s. The governor parameter in the simulation is the same as the values in the HPP during the measurement, which are the standard parameter settings EP1 in Vattenfall HPPs [13], as shown in Table 1. The values of the lag, the backlash and the delay are set to the recommended values, and remain constant throughout this study.

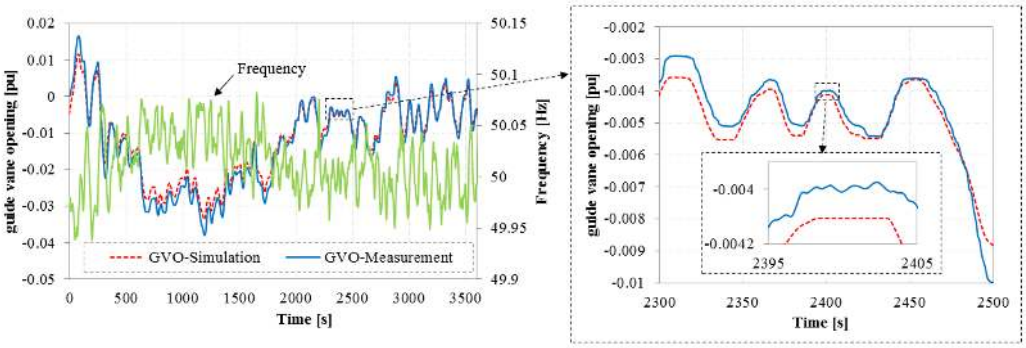

Figure 4. Comparison of the simulated GVO and the GVO measured in a Swedish HPP, the small plot inside the right figure demonstrates the measurement noise

Table 1. Values of parameters in the simulation for comparing to the measurement, the governor parameters b_p , K_p and K_i are the standard parameter settings EP1 in Vattenfall HPPs.

Parameter	b_p	K_p	K_i	Lag	Backlash	Delay
Value	0.04	1	5/12	0.25 s	0.00029 pu	0.097 s

As shown in Figure 4, the simulation has a good agreement with the measurement in time domain. However the most important focus in this study is the distance and amount of GV movements, and a comparison between the simulation and the measurement on these two indicators is necessary. During the 3885 s period, the distance and amount of GV movements calculated from the simulated GVO are 61.3 % stroke and 109; Nevertheless for the measured GVO, the value of these two indicators are 63.6 % stroke and 1858, which are strongly affected by the noise in the measurement data, especially the amount of movements. The small plot inside Figure 4 demonstrates the measurement noise, between 2395 s to 2405 s, the amount of movements in the measured GVO is far more than the simulated value.

A threshold is applied to solve the issue caused by the measurement noise. Any single movement, with its distance smaller than the threshold, is regarded as "a noise" instead of a small GV movement (skipped when calculating the amount and distance of movements). As demonstrated in Figure 5, larger thresholds leads to smaller values of the two indicators. The movement amount drops dramatically around 1.0 E-05, and Figure 4 shows that the scale of the "noise" is at least 1.0 E-05. Therefore, an initial selection of the threshold value is around 1.0 E-4, with an acceptable agreement between the simulation and the measurement in terms of the two indicators

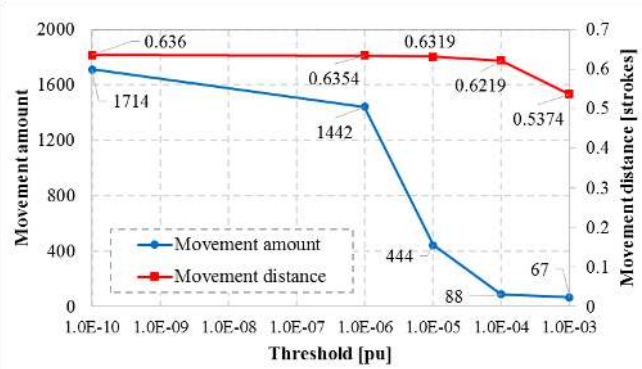

Figure 5. Distance and amount of movements calculated from the measured GVO during the 3885 s period under different values of threshold. (The simulated distance and amount of GV movements are 0.613 stroke and 109)

2.1.3 Model of the Nordic power system

Figure 6 shows a simple model of the Nordic power system [4,13], where all power plants are lumped into one, and the single power plant is adopting the investigated filters. The equations of the plant and grid are shown in (2) and (3) respectively, and the parameters of the model can be found in Table 2.

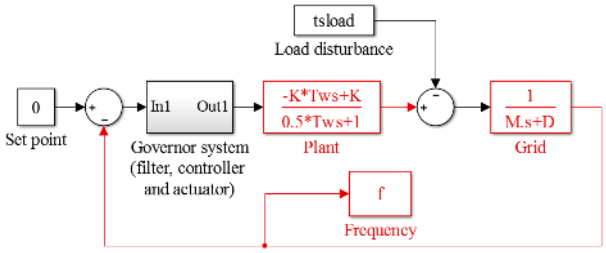

Figure 6 [4]. Simulink model of the Nordic power system, for computing the power system frequency

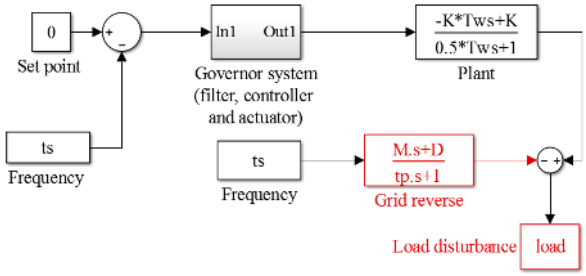

Figure 7 [4]. Simulink model of a " grid inverse" for computing the load disturbance

$$\text{Plant: } P(s) = K \cdot \frac{-T_w s + 1}{0.5 T_w s + 1} \quad [13] \tag{2}$$

$$\text{Grid: } G(s) = \frac{1}{Ms + D} \quad [13] \tag{3}$$

$$\text{Grid inverse: } G_r(s) = \frac{Ms + D}{t_p s + 1} \quad [4] \tag{4}$$

Table 2 [13]. Parameters of the plant and the grid

Symbol	Parameter	Value
K	Scaling factor	$10 \times b_p$ [pu]
T_w	Water time constant	1.5 [s]
M	System inertia	13 [s]
D	Load damping constant	0.5 [pu]

The influence of the different filters on the frequency quality of power systems can be simulated and compared by the power system model, based on a certain load disturbance. Nevertheless, the unknown load disturbance needs to be produced firstly from the existing measured frequency, by an "grid inverse" model [4] shown in Figure 7. The transfer function of the inverse grid model is described in (4). A pole with time constant t_p is applied to the grid inverse model to avoid high amplification of high frequency noise in the grid frequency signal, according to the theory of Internal Model Control [15]. Its value is set to 0.1 in this study. The computed load disturbance is presented and discussed in Section 2.1.4. It is worth clarifying that the two models presented in this Section 2.1.3 are from [4], and the main information is repeated here for reader's convenience. More details can be found in [4,13].

2.1.4 Measured one-month frequency data and computed load disturbance

The input of the governor model, for the long-term simulation of the GVO, is a sequence of one-month measured data of the frequency of Nordic power system. It was measured in Finland for December of 2012, the total data length is 2678400 s, and the sampling time is 1.0 s. As mentioned above, the input of the power system model shown in Figure 6, for the long-term simulation of the frequency, is a sequence of one-month load disturbance computed from the measured frequency by the model shown in Figure 7. The frequency and the load disturbance are presented in Figure 8, only one-day data (for December 1 in 2012) is plotted.

Besides, Figure 9 presents the result of Fast Fourier Transform (FFT) of the one-month grid frequency data. It is shown that there is a peak occurring at 0.0167 Hz that corresponds to 60 s, and this will be discussed in the theoretical analysis in Section 2.2.

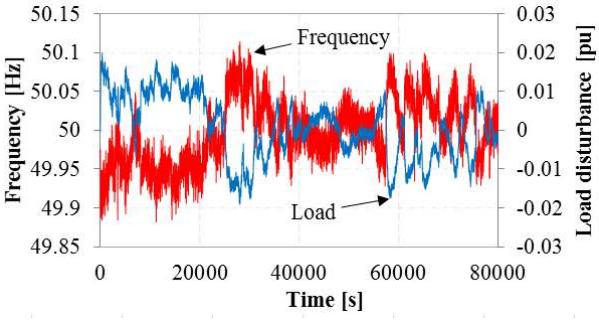

Figure 8. Time-domain illustration of the measured frequency and the computed load disturbance, only one-day data (for December 1 in 2012) is plotted

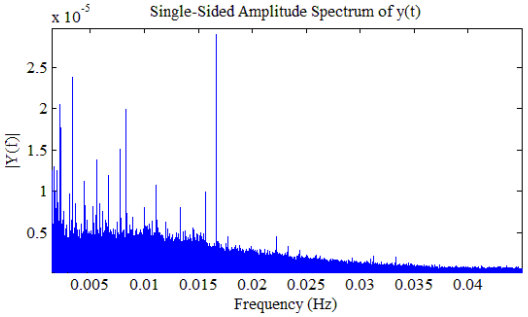

Figure 9. Single-sided amplitude spectrum of the one-month frequency data, the frequency for the highest peak is 0.0167 Hz.

2.2 Basic theoretical formulas

In [3], based on idealized frequency deviation signals $\Delta f = A_f \sin\left(2\pi t/T_f\right) = A_f \sin(\omega t)$, the following formula is proposed to estimate the accumulated movement distance (D_y):

$$D_y = 4 \cdot \frac{T_{total}}{T_f} G_{PI} \cdot G_m \cdot A_f \quad [3]. \tag{5}$$

In the equations, A_f is the amplitude of the sinusoidal input frequency signal, T_{total} and T_f represent the total time and a period respectively. G_{PI} is the gain of the PI controller and G_m is the product of the gains of mechanical components (dead zone and lag), as shown below:

$$G_{PI} = \frac{1}{b_p} \sqrt{\frac{1+\omega^2\left(K_p/K_i\right)^2}{1+\omega^2\left(\frac{1+b_pK_p}{b_pK_i}\right)^2}} \quad \text{[pu/ pu] [3]}, \tag{6}$$

$$G_{backlash} = 1 - \frac{B_y}{2A_{in}} \quad \text{[pu/pu] (if } A_{in} \geqslant B_y/2\text{) [3]}, \tag{7}$$

$$G_{lag} = \frac{1}{\sqrt{1+T_y^2\omega^2}} \quad [3]. \tag{8}$$

Here, A_{in} is the input amplitude, while B_y represents the bandwidth of backlash. T_y stands for the lag in the main servomotor.

However, in this study, the structure of the governor model is slightly different, as shown in Figure 10. The mechanical components are included in the feedback loop, therefore the transfer function is changed.

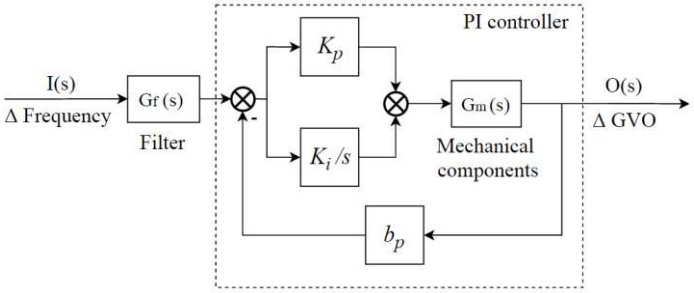

Figure 10. Block Diagram of the governor, with the mechanical components included in the feedback loop

The gain of the PI controller, $G_{PI\text{-}2}$, is described as

$$G_{PI-2}=\frac{1}{b_p}\sqrt{\frac{1+\omega^2\left(K_p/K_i\right)^2}{1+\omega^2\left(\frac{1/G_m+b_pK_p}{b_pK_i}\right)^2}}\text{, [pu/ pu] [3].} \tag{9}$$

Comparing to (6), the term G_m now is included in the gain of PI governor, but the value of the G_m is very close to 1.0 due to the small values of the lag (0.25 s) and the backlash (0.00029 pu). Therefore, in this study, the term G_m is ignored and the gain of PI governor still adopts (6).

The gains of different filters, G_f, are as shown in (10) through (12).

$$\text{Dead zone :}\quad G_{dz}=1-\left|\frac{E_{dz}}{A_{in}}\right|\text{, (if } |A_{in}|\geq|E_{dz}|\text{) [3]} \tag{10}$$

$$\text{Floating dead zone: } G_{fdz}=1-\frac{E_{fdz}}{2A_{in}}\quad\text{[pu/pu], (if } A_{in}\geqslant B_y/2) \tag{11}$$

$$\text{Linear filter:}\quad G_l=\frac{1}{\sqrt{1+T_f{}^2\omega^2}} \tag{12}$$

Equations (11) and (12) here are slightly revised based on (7) and (8), because the mathematical form of the floating dead zone and the first-order linear filter are equivalent to the backlash and the lag respectively.

Moreover, the nonlinearities can be linearized by describing functions [32] as well, therefore another set of formulas is obtained for the dead zone and the floating dead zone, as shown in (13) and (15), and they are also compared to (10) and (11) in the discussion of Section 3.

$$G_{dz-2}=N_{dz}=\frac{1}{\pi}\left[\pi-2\arcsin\left(\frac{E_{dz}}{A_{in}}\right)-2\left(\frac{E_{dz}}{A_{in}}\right)\sqrt{1-\left(\frac{E_{dz}}{A_{in}}\right)^2}\right]\text{ [4]} \tag{13}$$

$$N_{fdz}(A)=\frac{1}{\pi}\left[\frac{\pi}{2}+\arcsin\left(1-\frac{E_{fdz}}{A_{in}}\right)+\left(1-\frac{E_{fdz}}{A_{in}}\right)\sqrt{\frac{2E_{fdz}}{A_{in}}-\left(\frac{E_{fdz}}{A_{in}}\right)^2}\right]-j\frac{1}{\pi}\left[\frac{2E_{fdz}}{A_{in}}-\left(\frac{E_{fdz}}{A_{in}}\right)^2\right]=a+bj\text{ [4]} \tag{14}$$

$$G_{fdz-2}=\sqrt{a^2+b^2}\text{ , (a and b are real numbers in (14))} \tag{15}$$

Overall, in this study, the theoretical formula for the accumulated movement distance ($D_{y\text{-}2}$) is

$$D_{y\text{-}2}=4\cdot\frac{T_{total}}{T_f}\cdot A_f\cdot G_f\cdot G_{PI}\ . \tag{16}$$

It aims to reflect the influence of different governor parameters and filter settings. If the filter is not considered in the calculation, the value of G_f is set to 1.0.

Besides, the formula of response time [3,18]

$$T_r=\frac{1+b_pK_p}{b_pK_i}\left[1-\ln(1+b_pK_p)\right]\text{ [s] [3]} \tag{17}$$

is also applied in the later section, for indicating the impact of altering the governor parameters. T_r stands for the time it takes for the GVO to reach 63.2 % ($\approx$1-e^{-1}) of the final regulation after a step disturbance.

3. Results and discussions

In this section, distance and amount of GV movements, as well as the frequency quality, are simulated for one month under different governor parameters and filter settings. The two indicators of GV movements are computed by using the governor model in Figure 2, with the input that is the one-month measured frequency; the frequency quality is simulated by applying the Nordic power system model in Figure 6, with the input that is the one-month simulated load disturbance. The theoretical formula is also applied to calculate the distance and the results are compared to the simulations. The default parameters setting is the same as the values adopted in the on-site measurement, as shown in Table 1.

3.1 PI governor parameters

Table 3 shows the results of simulations and formula calculations under different values of K_p and K_i. The value of b_p is not altered, because it would affect the total amount of regulating strength in the system. There is a clear tendency that larger values of K_p and K_i lead to longer movement distance and shorter response time. The response time represents the regulation rapidity of the hydropower units, however a sharp decrease of the response time cannot obviously improve the frequency quality described by the mean value and standard deviation of the simulated frequency sequence. Another interesting result is that the movement amount is not always in positive correlation with the movement distance. The situation under parameter No. 5 is highly unfavourable, with a slow regulation response and largest movement amount.

Table 3. Results of one-month simulations and formula calculations under different governor parameters. In the column "50-Mean", the value 1.552E-04 Hz shows the mean value of the frequency is 49.9998448 Hz.

No.	K_p [pu]	K_i [s^{-1}]	Formula calculation		GV - Simulation		Frequency quality - Simulation	
			GV movement distance:$D_{y\text{-}2}$	Response time: T_r	Movement distance	Movement amount	50 - Mean	Standard deviation
1	1.0	0.417	243.7 strokes	60.0	245.8 strokes	73710	1.552E-04 [Hz]	0.0429 [Hz]
1	1.0	0.417	100.00%	100.00%	100.00%	100.00%	100.00%	100.00%
2	2.0	0.833	186.89%	49.88%	177.28%	122.12%	99.40%	96.39%
3	5.0	2.083	365.34%	19.64%	322.58%	167.28%	99.04%	94.87%
4	5.0	0.833	194.13%	49.10%	186.40%	179.89%	99.40%	95.28%
5	5.0	0.417	135.37%	98.20%	130.22%	210.81%	99.98%	97.71%
6	1.0	0.833	189.11%	50.00%	178.39%	110.75%	99.40%	98.37%

3.2 Filter parameters

Table 4 presents the results of simulations and formula calculations under different filter settings. The one-month simulations support the results in [4] from the one-day simulations: the floating dead zone outperforms the dead zone, with less GV movements and better frequency quality. The linear filter provides a relatively weak impact on both the wear reduction and the frequency quality. Although the dead zone leads to the worst frequency quality, the influence is actually not large with respect to the deviation of the mean value, which is smaller than 6.0E-4 Hz in all cases.

Table 4. Results of one-month simulations and formula calculations under different filter settings. In the column "50-Mean", the value 1.552E-04 Hz shows the mean value of the frequency is 49.9998448 Hz.

Filter type	Value setting [pu]	GV movement distance		GV - Simulation		Frequency quality - Simulation	
		Formula (10) or (11)	Formula (13) or (15)	Movement distance	Movement amount	50 - Mean	Standard deviation
No filter [abs]	\	\	\	245.8 strokes	73710	1.552E-04 [Hz]	0.0429 [Hz]
No filter [pu]	\	100%	100%	100.0%	100.0%	100.00%	100.0%
Dead zone (E_{dz})	±0.01%	90.00%	87.29%	90.4%	98.3%	156.92%	108.9%
	±0.02%	80.00%	74.71%	81.5%	95.6%	211.42%	117.9%
	±0.05%	50.00%	39.10%	56.8%	77.0%	385.53%	145.8%
Floating dead zone (E_{fdz})	2×0.01%	90.00%	95.49%	93.8%	81.4%	101.85%	103.7%
	2×0.02%	80.00%	88.15%	81.4%	63.7%	98.80%	109.7%
	2×0.05%	50.00%	59.27%	41.0%	19.6%	91.10%	133.8%
Linear filter (Tf1)	1.0	99.46%	\	99.3%	92.0%	100.02%	101.0%
	2.0	97.88%	\	98.1%	88.4%	100.05%	102.8%
	3.0	95.40%	\	96.5%	84.9%	100.09%	106.9%

3.3 Theoretical formulas

The aim of applying the theoretical formula (16) is not only to explain the influencing mechanism of different parameters, but also to achieve results, in a much simpler approach, to fit the long-term simulation based on real frequency measurement. In order to conduct the formula calculations, the amplitude (A_f) and period (T_f) of the input frequency signal $\Delta f = A_f \sin\left(2\pi t / T_f\right)$ need to be determined firstly. The period is selected as 60 s, because it is the typical period of the low frequency oscillation of the grid frequency, as shown in Figure 9 and in [19].

However, the values of the amplitude are different for analysing the PI governor parameters (Table 3) and the filter settings (Table 4). For calculating the results in Table 3, the amplitude only linearly affects the distance, hence it is tuned as 0.00035 pu (0.0175 Hz) by trial method to match the simulations. For the results in Table 4, the value of A_f also influence the gains of dead zone and floating dead zone, and 0.00035 pu is no longer suitable. Instead, the amplitude is tuned as 0.001 pu (0.05 Hz) to obtain a good agreement of simulations in terms of unified values. More specifically, with the 0.001 pu amplitude, the absolute movement distance without filters is 696.3 strokes, deviating from the simulation result (245.8 strokes).

As demonstrated in Table 3, the formula approximations under different PI governor parameters fit the simulations well, with the error less than 5.1%. As shown in Table 4, the formulas achieve an acceptable overall agreement with the simulations. For the dead zone, the simpler formula (10) has a better performance, while formula (13) from the describing function outperforms (15) in terms of the floating dead zone. It is worth emphasizing that the formula calculation based on the trial method and fitting strategies is not rigorous, however it is effective and efficient for tuning the governor parameters of the governor and filters, as long as the selection of amplitude (A_f) and period (T_f) of the input are reasonable.

4. Conclusions

In this study, regulation strategies to extend the service life of hydropower turbines are analysed, which is indicated by the distance and amount of GV movements. Firstly, a governor model is built and verified by on-site measurements in a Swedish HPP. Then, based on the governor model and models of the Nordic power system, long-term simulations (for one month) are conducted for analysing the GV movement and frequency quality of power systems. Besides, basic theoretical formulas are also applied and compared to the simulation results.

The conclusions are drawn as follows: (1) The proposed governor model is applicable, with a good agreement with the measurements. (2) For the PI governor parameters, larger values of K_p and K_i lead to longer movement distance and shorter response time, but the movement amount is not always in positive correlation with the movement distance. The impact of governor parameters on the frequency quality of power systems is relatively small, under the same b_p value. (3) For the filter settings, the conclusions drawn in [4] based on one-day simulations are validated by the one-month simulations in this study. The floating dead zone has the best overall performance, leading to less GV movements and good frequency quality. (4) The theoretical formulas can achieve acceptable predictions on distance of GV movements, based on the suitable selection of amplitude (A_f) and period (T_f) of the sinusoidal input frequency. This supplies a simple way of tuning both PI governor parameters and filter settings.

Acknowledgements

The authors thank the China Scholarship Council (CSC), StandUp for Energy, and Vattenfall. The research presented was also carried out as a part of "Swedish Hydropower Centre - SVC". SVC has been established by the Swedish Energy Agency, Elforsk and Svenska Kraftnät together with Luleå University of Technology, KTH Royal Institute of Technology, Chalmers University of Technology and Uppsala University (www.svc.nu). The authors also acknowledge the support from the National Natural Science Foundation of China under Grant No. 51379158.

References

[1] Doujak E 2014 Effects of Increased Solar and Wind Energy on Hydro Plant Operation. *Hydro Review Worldwide*:28-31

[2] Storli P and Nielsen T 2014. Dynamic load on a Francis turbine runner from simulations based on measurements. *Proc. IOP Conference Series: Earth and Environmental Science*, 22:032056

[3] Yang W, Norrlund P, Saarinen L, Yang J, Guo W and Zeng W 2016 Wear and tear on hydro power turbines–Influence from primary frequency control. *Renewable Energy* 87:88-95

[4] Yang W, Norrlund P, Saarinen L, Yang J, Zeng W and Lundin U Wear reduction for hydro power turbines considering frequency quality of power systems: a study on controller filters (to be published).
[5] Dorji U and Ghomashchi R 2014 Hydro turbine failure mechanisms: An overview. *Eng Fail Anal* 44:136-47
[6] Liu X, Luo Y and Wang Z 2016 A review on fatigue damage mechanism in hydro turbines. *Renewable and Sustainable Energy Reviews* 54:1-14
[7] Seidel U, Mende C, Hübner B, Weber W and Otto A 2014. Dynamic loads in Francis runners and their impact on fatigue life. *Proc. IOP Conference Series: Earth and Environmental Science*, 22:032054
[8] Trivedi C, Gandhi B and Michel CJ 2013 Effect of transients on Francis turbine runner life: a review. *Journal of Hydraulic Research* 51:121-32
[9] Gagnon M, Tahan S, Bocher P and Thibault D 2010. Impact of startup scheme on Francis runner life expectancy. *Proc. IOP Conference Series: Earth and Environmental Science*, 12:012107
[10] Huth H-J 2005 Fatigue design of hydraulic turbine runners. Norwegian University of Science and Technology
[11] Wurm E 2013. Consequences of primary control to the residual service life of Kaplan runners. *Proc. Russia Power 2013 & Hydrovision Russia 2013*, Moscow, Russia
[12] Momcilovic D, Odanovic Z, Mitrovic R, Atanasovska I and Vuherer T 2012 Failure analysis of hydraulic turbine shaft. *Eng Fail Anal* 20:54-66
[13] Saarien L 2014 A hydropower perspective on flexibility demand and grid frequency control. Uppsala University, Uppsala
[14] 2011 IEEE Guide for the Application of Turbine Governing Systems for Hydroelectric Generating Units. *IEEE Std 1207-2011 (Revision to IEEE Std 1207-2004)*:1-131
[15] Ljung L and Glad T 2000 Control theory-multivariable and nonlinear methods. (Taylor and Francis)
[16] Ghrist III WD 1986 Floating deadband for speed feedback in turbine load control. *Patent No. US 4593364 A*
[17] Hägglund T 2013 A unified discussion on signal filtering in PID control. *Control Engineering Practice* 21:994-1006
[18] Yang W, Yang J, Guo W and Norrlund P 2016 Response time for primary frequency control of hydroelectric generating unit. *International Journal of Electrical Power & Energy Systems* 74:16-24
[19] Grøtterud M 2012 Analysis of the Slow Floating in Grid Frequency of the Nordic Power System: Impact of Hydraulic System Characteristics. Norwegian University of Science and Technology